# Evolution of a barotropic shear layer into elliptical vortices

Anirban Guha,* Mona Rahmani, and Gregory A. Lawrence
*Department of Civil Engineering, University of British Columbia,Vancouver, Canada V6T 1Z4.*
(Dated: October 12, 2012)

Barotropic shear layers, on becoming unstable, produce the well known Kelvin-Helmholtz instability (KH). The nonlinear manifestation of KH is usually in the form of spiral billows. However, a piecewise linear shear layer produces a different type of KH characterized by elliptical vortices of constant vorticity connected via thin braids. Using DNS and Contour Dynamics, we show that the interaction between two counter-propagating vorticity waves are solely responsible for this KH formation. We investigate the rotation and nutation of the elliptical vortex, and the oscillation and straining of the braids. Our analysis also provides possible explanation behind the formation and evolution of elliptical vortices appearing in geophysical and astrophysical flows, e.g. meddies, Jovian vortices, Neptune's Great Dark Spot, coherent vortices in the wind belts of Uranus, etc.

PACS numbers: 47.20.Ft, 47.32.C-, *92.10.hf, 47.15.ki



## I. INTRODUCTION

Barotropic shear layers are ubiquitous in the atmosphere and oceans. These layers can become hydrodynamically unstable, giving rise to an instability mechanism widely known as the Kelvin-Helmholtz instability (KH). The non-linear manifestation of KH is usually in the form of spiralling billows, breaking of which generates turbulence and subsequent mixing in geophysical flows.

In theoretical and numerical studies, the hyperbolic tangent velocity profile ($U(y) = \tanh(y)$) is often considered to be the prototype of smooth barotropic shear layers [1]. Initially interested in understanding the long time evolution of KH emanating from this profile, we have performed a moderate Reynolds number Direct Numerical Simulation (DNS); see Fig. 1(a). The flow re-laminarizes once the KH billow completely breaks down into smallest scales via turbulent processes. At this stage the shear layer is much sharper and around four times thicker than the initial $\tanh(y)$ profile. This four-fold increase in thickness also leads to an equal increase in the flow Reynolds number, making the flow more inviscid. Moreover, the shear layer profile at this stage closely matches the piecewise linear profile (see Fig. 1(b,c)):

$$U(y) = \begin{cases} 1 & y \geq 1 \\ y & -1 \leq y \leq 1 \\ -1 & y \leq -1 \end{cases} \tag{1}$$

Here $U$ is the non-dimensional velocity of the shear flow. Eq. (1) now becomes the new base flow and serves as the initial condition for the subsequent instability processes.

The linear stability analysis of the base flow given by Eq. (1) dates back to Lord Rayleigh [2]. The first nonlinear analysis however was performed more than a century later. Using a boundary integral method known as the *Contour Dynamics*, Pozrikidis and Higdon [3] showed that the piecewise linear shear profile evolves into nearly elliptical patches of constant vorticity - *Kirchhoff vortices*. We hypothesize that the initial shear layer profile determines the asymptotic form of the ensuing KH - smooth shear layers give rise to spiral billows, while sharp shear layers produce Kirchhoff vortices.

The spiralling billow form of KH has been thoroughly investigated in the past. In fact, the spiral billow shape has become the signature of KH [4]; but little is known about the non-linear evolution of the sharp shear layer. This is because the piecewise linear profile is usually considered to be of little practical relevance. Its usage is therefore restricted to theoretical studies, mainly as a crude approximation of smooth shear layers [5, 6]. However, our DNS results in Fig. 1(a,b) indicate otherwise - the sharp profile can also occur in nature. The fact that this profile produces elliptical vortices similar to those observed in geophysical and astrophysical flows, e.g. meddies in Atlantic ocean [7], Neptune's Great Dark Spot [8], coherent vortices in the atmosphere of Jupiter and Uranus [9], has motivated us to investigate further.

## II. LINEAR THEORY

In 1880, Lord Rayleigh [2] performed a linear stability analysis of the shear layer profile in Eq. (1) and showed it to be unstable for the range of wavenumbers $0 \leq \alpha \leq 0.64$, the fastest growing mode being $\alpha_{crit} = 0.4$. In the conventional linear stability approach, infinitesimal wavelike perturbations are superimposed on a laminar background flow and an eigenvalue problem is solved to find the band of unstable wavenumbers [10]. This mathematical exercise, however, provides little insight into the underlying physical mechanism. In the past 50 years there has been a continuous effort to provide a mechanistic picture of hydrodynamic instabilities, especially homogeneous and stratified shear instabilities. Analytical studies performed on the profile in Eq. (1) have shown that the interaction between two vorticity waves

* aguha@mail.ubc.ca; Also at Institute of Applied Mathematics, University of British Columbia,Vancouver, Canada V6T 1Z2.

is responsible for the development of KH [6, 11–16]. We refer to this wave interaction based interpretation of hydrodynamic stability as the "Wave Interaction Theory" (WIT).

KH can be understood in the light of WIT by referring to Eq. (1). The vorticity $\Omega \equiv dU/dz$ is discontinuous at $z = \pm 1$, which allows each of these two locations to support a *stable*, progressive, interfacial wave called the vorticity wave (also known as the Rayleigh wave). In rotating frame, its analogue is the Rossby edge wave which exists at the discontinuities in Potential Vorticity. In general, a vorticity wave at the interface $z = z_j$ has a phase speed $c_r(z_j)$ given by

$$c_r(z_j) = U(z_j) + c_r^{int}(z_j) \tag{2}$$

The first component, $U(z_j)$, is the background velocity, while $c_r^{int}(z_j)$ is the intrinsic phase speed defined as

$$c_r^{int}(z_j) = \frac{[\Omega]_{z_j}}{2\alpha} \tag{3}$$

where $[\Omega]_{z_j} = \Omega(z_j + \epsilon) - \Omega(z_j - \epsilon)$ is the jump in $\Omega$ across $z_j$. For the profile in Eq. (1), the arrangement is such that $c_r^{int}(z_j)$ is always directed counter to $U(z_j)$. We define such waves as counter-propagating vorticity waves (CVWs) (analogous to counter-propagating Rossby waves in a rotating frame). The CVWs at $z = \pm 1$ have [15]:

$$c_r^{\pm} \equiv c_r(\pm 1) = \pm 1 \mp \frac{1}{2\alpha} \tag{4}$$

The above equation implies that these two waves always travel in opposite directions. The wave at $z = 1$ is left moving while the one at $z = -1$ moves to the right. Although each of them is stable, their interaction can lead to instability, producing KH.

Consider a pair of CVWs:

$$\eta^+ = a_0 \cos(\alpha x - \Phi) \qquad \text{at } z = 1 \tag{5}$$
$$\eta^- = a_0 \cos(\alpha x) \qquad \text{at } z = -1 \tag{6}$$

where the perturbation amplitude $a_0 \ll 1$ and the phase shift $\Phi \in [-\pi, \pi]$. *Modal growth* occurs only when the two waves together behave like a normal mode. Two conditions need to be precisely satisfied for modal growth: (a) *phase locking* - the waves are stationary relative to each other, i.e. $c_r^+$ and $c_r^-$ become zero after interaction, and (b) *mutual growth* - the phase shift between the waves is such that one makes the other grow exponentially. Linear theory predicts this phase shift to be $\Phi^{modal} = \cos^{-1}\left\{(1-2\alpha)\, e^{2\alpha}\right\}$ [3]. For $\alpha = \alpha_{crit}$, the corresponding $\Phi_{crit}^{modal} = 0.353\pi$. Thus WIT provides the appropriate initial conditions (i.e. $\alpha_{crit}$ and $\Phi_{crit}$) for modelling the non-linear evolution.

Unfortunately, WIT itself is limited to the *linear* regime only. Current methodology does not allow a straightforward non-linear extension. This is a direct consequence of linearization which forces the vorticity interfaces to become vortex sheets [6, 11, 16]. Therefore it is questionable whether *non-linear* evolution KH can be understood in terms of two interacting non-linear vorticity waves.

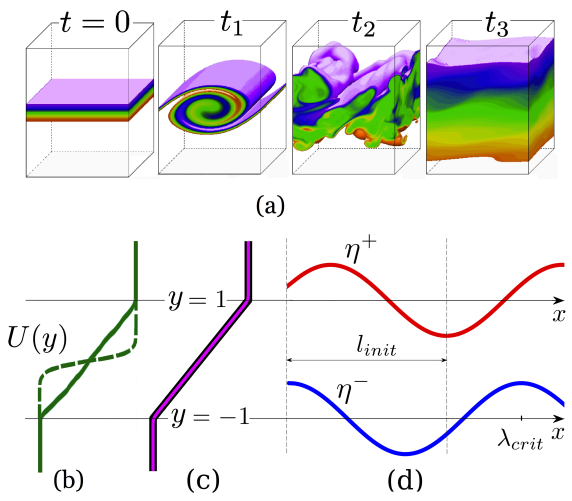


FIG. 1. (a) 3D DNS at $Re = 2400$ performed to capture the complete turbulent dissipation of a KH billow ensuing from an initial flow given by $U(y) = \tanh(y)$. False colour is added to aid visualization. (b) The dashed line represents the initial velocity profile, while the solid line shows the velocity profile once the flow re-laminarizes ($t = t_3$). (c) The Magenta line is the continuous velocity profile obtained from Eq. (8), while the thick black line below it is the piecewise linear profile from Eq. (1). Both of them closely mimic the solid green line. (d) Linear vorticity waves (exaggerated) existing at the vorticity discontinuities.

## III. NON-LINEAR FORMULATION

Over the last few decades, sophisticated computational techniques have been developed for precise understanding of turbulent processes. Two such techniques worth mentioning are Direct Numerical Simulation (DNS) and vortex methods.

Many geophysical and astrophysical flows can be assumed incompressible and quasi-inviscid (involve high Reynolds number). In such flows, non-linear processes like chaos and turbulence are solely driven by vortex interactions [17]. Vortex methods are especially useful under such circumstances; they numerically solve the inviscid and incompressible Navier-Stokes equations (Euler equations). An example of one such 2D vortex method is Contour Dynamics [18].

### A. Contour Dynamics

High Reynolds number flows have a tendency to develop Finite Area Vortex Regions (FAVR) with steep sides [18]. If the flow is incompressible and 2D, the area

as well as the vorticity of an FAVR are conserved quantities. The contour (FAVR or "vortex patch" boundary) is basically a vorticity jump and a material surface [17]. Substantial simplification is possible for constant vorticity patches; the governing 2D Euler equations can be reduced to a 1D boundary integral. This provides a significant computational advantage of computing the evolution of an FAVR by only solving the contour motion. This methodology is known as the Contour Dynamics (CD). Numerical implementation of CD is done in a Lagrangian framework by tracing the contour with a set of $N$ marker points.

Observing that a piecewise linear shear layer can be represented by a horizontally periodic patch of constant vorticity, Pozrikidis and Higdon [3] have used CD to simulate the non-linear evolution process. The evolution of the $i$-th Lagrangian marker is given by [5] :

$$\frac{d\mathbf{x}_i}{dt} = -\frac{\Omega}{4\pi}\int_C \ln\left[\cosh\left(\alpha\triangle y_i^{'}\right) - \cos\left(\alpha\triangle x_i^{'}\right)\right] d\mathbf{x}^{'} \quad (7)$$

where $\Omega = 1$, $\mathbf{x} = [x, y]^T$, $\triangle x_i^{'} = x_i - x^{'}$, $\triangle y_i^{'} = y_i - y^{'}$ and $C$ is the contour around one patch. On perturbing the contour with sinusoidal disturbances, the shear layer rolls up producing nearly elliptical patches of constant vorticity [3]. Thus we infer that *the contour is not just a material boundary, it is actually a pair of interacting CVWs.*

To elucidate this point further we refer to WIT which explains how the interaction between two CVWs, each existing at a vorticity discontinuity, *solely* governs the (linear) evolution of a piecewise linear shear layer. Likewise, CD simulation has shown that the shear layer contour (like CVWs, the shear layer contour also exists at the vorticity discontinuities) is *solely* responsible for the (non-linear) evolution of a piecewise linear shear layer. It follows that the shear layer contour and the pair of CVWs are one and the same thing. This observation has another important implication - CD acts as a non-linear extension of WIT. Thus the shortcomings of WIT arising from linearization can be avoided, making it possible to understand the non-linear evolution of KH in terms of two interacting CVWs.

We perform a CD simulation with initial condition based on WIT; we choose $\alpha = \alpha_{crit}$ and $\Phi = \Phi_{crit}^{modal}$, and initialize the problem using Eqs (5)-(6). This allows us to simulate the non-linear evolution of the fastest growing mode of KH arising in a piecewise linear shear layer. Considering a domain one wavelength ($\lambda_{crit} \equiv 2\pi/\alpha_{crit} = 5\pi$) long, we solve Eq. (7) using central differencing for space derivatives and $4^{\text{th}}$ order Runge-Kutta for time. Each wave is initially represented by 400 points. During its evolution process, an adaptive point insertion-deletion algorithm is used to check if the neighbouring points are within a desired distance.

Pozrikidis and Higdon [3] studied the nonlinear evolution of a piecewise linear shear layer subject to different types of initial disturbances, i.e. different combinations of wavenumbers ($\alpha$) and phase shifts ($\Phi$). For each initial condition, the shear layer evolved into a corresponding nonlinear state. Since the wavenumber of maximum growth ($\alpha_{crit}$) usually determines the non-linear state of a shear layer, it is unlikely to physically observe most of the non-linear states depicted in Pozrikidis and Higdon.

### B. Direct Numerical Simulation

Previous studies have used CD mainly as a tool for *qualitative* understanding of problems involving inviscid vortical flows [19]. In order to demonstrate the quantitative capabilities of CD, we validate our CD simulation against a pseudo-spectral Direct Numerical Simulation (DNS). We also expect that DNS will provide a parallel understanding of the phenomena. The DNS code uses full Fourier transform in the horizontal direction, and half-range sine or cosine Fourier transform in the vertical direction in order to convert the set of partial differential equations (Navier-Stokes equations) into ordinary differential equations. Time integration is performed using a third-order Adams-Bashforth method. Detailed description of this code can be found in the work of Winters et al. [20].

We consider a domain of length $\lambda_{crit}$ in the horizontal direction and nine times the initial shear layer thickness in the vertical direction. The horizontal boundary condition is periodic while the vertical boundary condition is no-flux free-slip. We perform a 2D simulation at Reynolds number $Re = 10,000$ ($Re = 1/\nu$, where $\nu$ is the fluid viscosity). At such high $Re$, DNS provides a good representation of CD. Our simulation is resolved using $2880 \times 3456$ points, which is fine enough to simulate the smallest scales of the 2D flow. Since non-differentiable profiles like Eq. (1) cause numerical issues (Gibbs phenomena), we use a smooth velocity profile that resembles the piecewise linear profile accurately; see Fig. 1(c). This velocity profile is derived from a vorticity distribution having the form

$$\Omega(y) = \frac{1}{2}\left[1 - \tanh\left(\frac{y^2 - 1}{\epsilon}\right)\right] \quad (8)$$

Integrating Eq. (8), the velocity profile is obtained directly: $U = \int \Omega dy$. The linear stability characteristic of this profile matches almost exactly with the piecewise profile, and has the same $\alpha_{crit}$. Equating the total circulation of DNS with CD yields $\epsilon = 0.100$. The vorticity field in DNS is perturbed to match the initial wave amplitude growth in CD.

## IV. RESULTS AND DISCUSSION

### A. Pre-saturation and Saturation Phases

The non-linear evolution of KH is illustrated in Fig. 2. It shows the vorticity field from DNS and contour lines

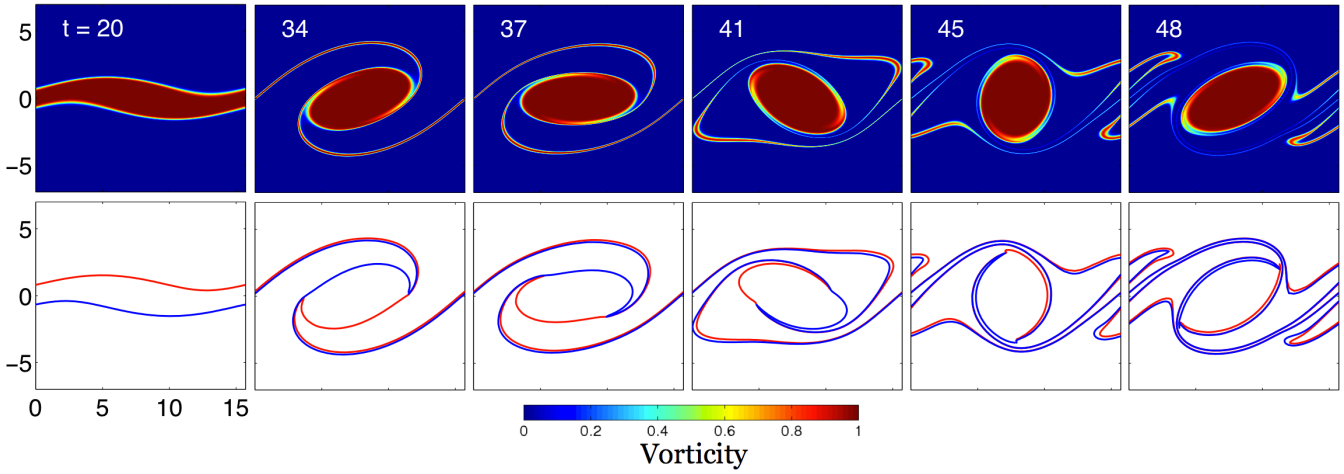


FIG. 2. Time evolution of Kelvin-Helmholtz instability - comparison between DNS (top) and CD (bottom).

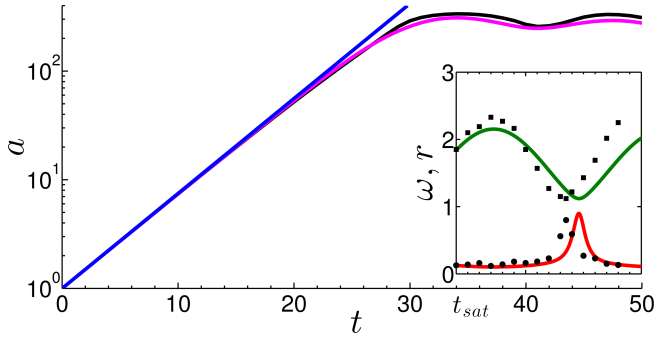


FIG. 3. Temporal variation of the wave amplitude $a$. The blue line is the prediction from linear theory, the black line corresponds to CD while the magenta line represents DNS results. The inset shows the variation of the ellipse aspect ratio $r$ (green line) and the angular rotation rate $\omega$ (red line) with time, obtained by solving Eqs. (10)-(11). The black markers indicate the data points measured from DNS.

from CD. Vorticity of the region enclosed by the contour lines is conserved in CD. However the presence of viscosity makes conservation of vorticity invalid in DNS. The implementation of high $Re$ DNS minimizes the viscous effects, making DNS comparable to CD. The basic premise behind our simulations is the conservation of total circulation $\Gamma = \Omega A$ (where the vorticity $\Omega = 1$ and $A$ is the shear layer area), which comes from Kelvin's Circulation theorem [17]. Its corollary is the conservation of shear layer area - a quantity that remains fixed at its initial value $A = 2\lambda_{crit}$.

Fig. 3 shows the time evolution of the wave amplitude, $a$. The maximum shear layer thickness, $H = 2(1 + a)$ evolves in a fashion similar to the wave amplitude $a$. We find the growth to be exponential, at least for $t \lessapprox 20$. CVW interaction causes the shear layer to grow nonlinearly. This phenomenon leads to the roll-up and formation of the elliptical core vortex (Kirchhoff vortex). The evolution process is shown in Fig. 2. The part of the shear layer between the crest of the lower wave and the trough of the upper wave (see Fig. 1(d)) gives rise to the elliptical core, the initial length of which is given by

$$l_{init} = \left(1 + \frac{\Phi_{crit}^{modal}}{\pi}\right) \frac{\lambda_{crit}}{2} \tag{9}$$

The flow saturates (i.e. the amplitude reaches a maxima) at $t_{sat} = 34$. For $t \geq t_{sat}$, approximately 80% of $\Gamma$ is concentrated in the core. H also reaches a maxima at saturation, and has the value $H_{max} = 8.7$. The fully formed elliptical cores are connected by thin filaments of fluid called *braids*. These braids wrap around the rotating cores, producing a complex spiral like structure, as shown in Fig. 2.

### B. Early Post-saturation Phase

After saturation, the core rotates with an angular velocity $\omega$, causing the wave amplitude, a, to oscillate with a time period $T_{amp} \approx 13$; see Fig. 3. The core also nutates, i.e. the core aspect ratio $r$ (defined as the ratio between the ellipse major axis and the minor axis) undergoes a periodic oscillation. This phenomenon is called *nutation* and is apparent from both Figs. 2 and 3.

#### 1. *Nutation*

To better understand the nutation process, we consider the simple model proposed by Kida [21]. An isolated Kirchhoff vortex rotates in the presence of a constant background strain-rate $\gamma$. The velocity field associated with this strain-rate is given by $u_s = \gamma\sigma$, $w_s = -\gamma\xi$ where $\sigma$ and $\xi$ are the principal axes with the origin at the centre of the ellipse. In our case, this velocity field mimics the leading order straining effect induced by the rotation of other Kirchhoff vortices. Note that the periodic

boundary condition takes into account the effects of the other Kirchhoff vortices. Let the clockwise angle between $\sigma$ and the ellipse major axis be $\theta$ at any instant. Then $\theta$ and $r$ evolve as follows [21]:

$$\omega \equiv \frac{d\theta}{dt} = -\gamma\left(\frac{r^2+1}{r^2-1}\right)\sin(2\theta) + \frac{\Omega r}{(r+1)^2} \quad (10)$$

$$\frac{dr}{dt} = 2\gamma r\cos(2\theta) \quad (11)$$

Eq. (11) implies that the nutation is caused by strain. It also reveals that $r$ reaches maxima at $\theta = \pm\pi/4$. Simultaneously, Fig. 2 shows that the core nutates with a maximum value of $r$ along the $x$ axis and a minimum along the $y$ axis. Therefore the $\sigma$ axis must make an angle $\pi/4$ with the $x$ axis. The angle made by the braid with the $x$ axis at the stagnation point(s) is also $\pi/4$. This is because the braid aligns itself with the streamlines.

To answer why the $\sigma$ axis makes an angle of $\pi/4$ with the $x$ axis, we consider an ideal problem where an infinite number of Kirchhoff vortices, each of circulation $\Gamma_{core} = \Gamma$ (note $\Gamma = 2\lambda_{crit}$), are placed along the $x$ axis with a constant spacing $\lambda_{crit}$ between their centres. The effect of a vortex patch at a point outside its own boundary is exactly the same as that of a point vortex of equivalent strength placed at the center of the patch [5]. Therefore we replace all the Kirchhoff vortices with point vortices of strength $\Gamma_{core}$. This provides a simplistic understanding of the mechanism by which the rotation of distant vortex patches strain a given patch. We find this *ideal* strain-rate to be

$$\gamma' = \frac{\Gamma_{core}}{2\pi\lambda_{crit}^2}\sum_{n=-\infty,n\neq 0}^{\infty} n^{-2} = 0.067 \quad (12)$$

The principal axes of the strain field produced by this infinite array of point vortices make angles of $\pm\pi/4$ with the $x$ axis. Hence, this ideal strain field and the strain field of our actual problem have the same orientation. Before comparing the magnitudes of these two fields, it is important to note that the presence of the braids complicate the actual problem by making the strain-rate magnitude vary spatially. We simplify the analysis by assuming a strain field of constant magnitude acting on the elliptical core, thereby reducing the problem to the Kida problem described by Eqs. (10)-(11). DNS is used to supplement the analysis by providing the values of $r$ and $\theta$ wherever necessary. By applying this methodology, the magnitude of the actual strain-rate is found to be $\gamma = 0.073$, which is quite close to the ideal value of 0.067 obtained from Eq. (12).

We also capture the evolution of $r$ and $\omega$ by solving Eqs. (10)-(11); see Fig. 3. The initial values are obtained from DNS, and $\gamma = 0.073$. The spike in $\omega$ at $t \approx 45$ is caused by $r \to 1$. The data points measured from DNS when compared with the Kida theory reveal that the latter can provide encouraging predictions. The nutation period is found to be $T_{nut} \approx 13$, while the period of core rotation is $T_{core} = 2\pi/\bar{\omega} \approx 26$ (overbar denotes average). $T_{core} \approx 2T_{nut}$ is because one full rotation corresponds to passing the coordinate axes twice. Likewise, $T_{core} \approx 2T_{amp}$ because the braids are connected to the two ends of the core.

#### 2. *Small Length Scale Production*

The smallest length scales are found to occur in the braid region adjacent to the core; see Fig. 2. This is due to the straining effect of the rotating elliptical core which causes the braid region in its vicinity to thin exponentially fast. In real flows, when a fluid element becomes sufficiently thin, the balance between the strain-rate and the viscous dissipation determines the small length scales. The order of magnitude of the core rotation induced strain-rate, $\gamma_{local}$, can be obtained by replacing the core with a point vortex of equivalent strength and located at the ellipse centre:

$$\gamma_{local} \sim \frac{\Gamma_{core}}{2\pi l^2} = \frac{1}{2} \quad (13)$$

where $l$ is the characteristic length of the core. Notice that this local strain-rate is one order of magnitude greater than the background strain-rate $\gamma$ or $\gamma'$.

The smallest length scale appearing in a 2D turbulent flow is $L_{2D} \sim Re^{-1/2}$ [22]. This length scale is a 2D analogue of the Taylor microscale occurring in 3D turbulent flows. In order to estimate the time when $L_{2D}$ appears in our flow, we formulate a braid evolution equation similar to Eq. (2.8) of Corcos and Sherman [23]:

$$\delta^2(t^*) = \delta^2(0)\,e^{-2\gamma_{loc}t^*} + \frac{\pi}{2\gamma_{loc}Re}\left(1 - e^{-2\gamma_{loc}t^*}\right) \quad (14)$$

where $\delta(t^*)$ is the braid thickness adjacent to the core at time $t^* = t - t_{sat}$. We estimate $\delta(0)$ from DNS and solve Eq. (14). We find that $L_{2D}$ appears soon after the saturation, around $t^* \approx 4$, implying that 2D transitional flows like KH can give rise to "turbulent" features at a very early stage.

### C. Late Post-saturation Phase

For $t \gtrapprox 50$, the core surface develops progressive vorticity waves. These are called the Kelvin $m$-waves or the Love $m$-waves [24], where $m$ is the eigenmode. In the absence of strain, $r < 3$ is the condition for stability of a Kirchhoff vortex [17]. Although $r$ satisfies this condition in our case (refer to the inset in Fig. 3), the presence of strain adds instability [25]. Finite amplitude $m = 4$ waves give rise to winding filaments, see Fig. 4. This is a feature of Kirchhoff vortices in background shear or strain, which has been thoroughly investigated by Dritschel [25]. Background shear or strain is however not necessary to produce winding filaments. Similar winding features are also seen in large aspect ratio Kirchhoff vortices even in the absence of shear or strain [24].

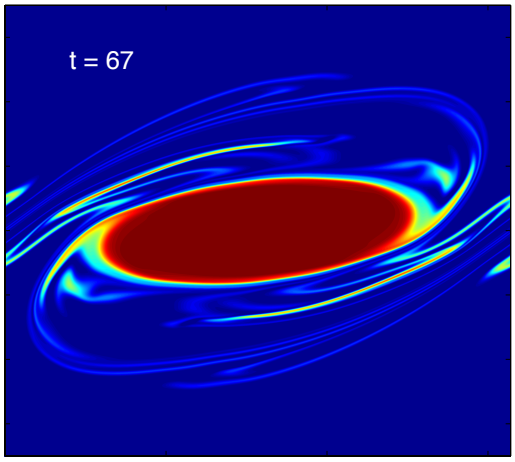


FIG. 4. Formation of winding filaments around the elliptical vortex during the late post-saturation phase.

## V. PRACTICAL IMPLICATIONS

In this Section we discuss several practical aspects of our work. The elliptical core shown in our simulations is a common feature in geophysical and astrophysical flows, e.g. coherent vortices in the wind belts of Uranus [9], Mediterranean eddies or meddies [7], vortices in Jupiter [8, 9], the Great Dark Spot of Neptune (which has disappeared now) [8], etc.

The wind belts of Uranus often produce an array of coherent elliptical vortices, see Fig. 3 of Liu and Schneider [9]. The probable mechanism behind the formation of the Uranian vortices, as suggested by our CD and DNS simulations, is the interaction of counter-propagating Rossby waves. Two dimensional CD and DNS modelling with streamwise periodic boundary condition can be justified in this context which implies that our simulations can provide a good description of the Uranian vortex dynamics. However, an added background shear present in the wind belts of Uranus slightly complicates the problem. The effect of this added shear can be incorporated in CD, DNS and the Kida model, making the subsequent analysis a straightforward extension of our present study.

The Great Red Spot and the White Oval BC of Jupiter, and the Great Dark Spot of Neptune can be well approximated as Kirchhoff vortices in a uniform background shear [8]. The rotation and nutation of these vortices were analyzed by Polvani et al. [8] using the Kida model. We hypothesize that Jovian and Neptunian vortices are produced by the interaction of counter-propagating Rossby waves in a fashion which is similar to the Uranian vortices.

Elliptical vortices known as the *meddies* are found in the region where Mediterranean sea meets the Atlantic ocean. The genesis of meddies is highly speculative; one possible explanation is the interaction of counter-propagating Rossby waves. This is corroborated by the observations near Portimão Canyon and Cape St. Vincent [7]. It is possible that the meddies, like Uranian and other giant planetary vortices, are also a non-linear manifestation of KH ensuing from sharp shear layers.

The average diameter of a meddy is $25-100$ km which is approximately half of the most unstable wavelength of the Rossby edge waves [7]. A simple visual inspection of Fig. 2 corroborates this observation. During its evolution process, meddies are found to produce winding filaments [26], similar to what we observe in Fig. 4. However for proper understanding of meddy evolution, density stratification, three dimensionality and aperiodic streamwise boundary condition should be taken into consideration.

## VI. CONCLUSION

A piecewise linear shear layer becomes unstable and evolves into a series of elliptical vortices of constant vorticity (Kirchhoff vortices) connected by thin braids. The interaction between two counter-propagating vorticity waves is the driving mechanism behind this instability process. Although this fact was known previously, linearized approximations forced the analysis to be valid only in the linear regime. By finding and exploiting the link between two quite different theories, namely the Wave Interaction Theory and the Contour Dynamics, we are able to extend the analysis to the fully non-linear domain.

The production of Kirchhoff vortices clearly indicates that KH arising from a piecewise linear shear layer is very different from the classical spiralling billow type KH ensuing from a smooth shear layer. The characteristics of this little known KH have been investigated. The rotation and nutation of the Kirchhoff vortices are found to be consistent with the predictions of Kida. The time period of rotation of the vortices is found to be twice the period of nutation and the period of maximum shear layer height oscillation. The braids connecting the Kirchhoff vortices rapidly thin to a length scale which is the 2D equivalent of Taylor microscale.

Elliptical vortical structures, similar to those found in our simulations, are quite common in nature, especially in regions with sharp shear. Examples of such vortices include meddies, Jovian vortices, Neptune's Great Dark Spot, coherent vortices in the wind belts of Uranus, etc. Our analysis can help understanding their formation and evolution process, motivating further investigation.

## ACKNOWLEDGMENTS

The authors would like to thank Dr. Neil Balmforth and Dr. Jeff Carpenter for their insightful comments. Thanks to Dr. Kraig Winters for the DNS code and WestGrid for providing computational support.

[1] P. Hazel, J. Fluid Mech. **51**, 39 (1972)
[2] J. Rayleigh, Proc. Lond. Math. Soc. **12**, 57 (1880)
[3] C. Pozrikidis and J. J. L. Higdon, J. Fluid Mech. **157**, 225 (1985)
[4] M. Rahmani, *Kelvin-Helmholtz instabilities in sheared density stratified flows*, Ph.D. thesis, The University of British Columbia, Vancouver (October 2011)
[5] C. Pozrikidis, *Introduction to Theoretical and Computational Fluid Dynamics*, first edition ed. (Oxford University Press, 1997)
[6] J. R. Carpenter, E. Tedford, E. Heifetz, and G. Lawrence, Appl. Mech. Rev. (to be published)(2012)
[7] L. M. Chérubin, N. Serra, and I. Ambar, J. Geophys. Res. **108**, 3058 (2003)
[8] L. Polivani, J. Wisdom, E. DeJong, and A. Ingersoll, Science **249**, 1393 (1990)
[9] J. Liu and T. Schneider, J. Atmos. Sci. **67**, 3652 (2010)
[10] P. Drazin and W. Reid, *Hydrodynamic Stability*, second edition ed. (Cambridge University Press, 2004)
[11] J. Holmboe, Geofys. Publ. **24**, 67 (1962)
[12] F. P. Bretherton, Q. J. Roy. Meteor. Soc. **92**, 335 (1966)
[13] R. Cairns, J. Fluid Mech. **92**, 1 (1979)
[14] B. Hoskins, M. McIntyre, and A. Robertson, Q. J. Roy. Meteor. Soc. **111**, 877 (1985)
[15] C. Caulfield, Journal of Fluid Mechanics **258**, 255 (1994)
[16] P. Baines and H. Mitsudera, J. Fluid Mech. **276**, 327 (1994)
[17] P. Saffman, *Vortex Dynamics*, first edition ed. (Cambridge University Press, 1995)
[18] G. S. Deem and N. J. Zabusky, Phys. Rev. Lett. **40**, 859 (Mar 1978)
[19] D. I. Pullin, Annu. Rev. Fluid Mech. **24**, 89 (1992)
[20] K. Winters, J. MacKinnon, and B. Mills, J. Atmos. Ocean. Tech. **21**, 69 (2004)
[21] S. Kida, J. Phys. Soc. Jpn. **50**, 3517 (1981)
[22] P. Davidson, *Turbulence: an introduction for scientists and engineers* (Oxford University Press, USA, 2004)
[23] G. M. Corcos and F. S. Sherman, J. Fluid Mech. **73**, 241 (1976)
[24] T. B. Mitchell and L. F. Rossi, Phys. Fluids **20**, 054103 (2008)
[25] D. G. Dritschel, J. Fluid Mech. **210**, 223 (1990)
[26] C. Ménesguen, B. Hua, X. Carton, F. Klingelhoefer, P. Schnürle, and C. Reichert, Geophysical Research Letters **39**, L05604 (2012)